International Journal of Engineering & Applied Sciences (IJEAS)
Vol.17, Issue 4 (1774094) 197-212
http://dx.doi.org/10.24107/ijeas.1774094
Int J Eng Appl Sci 17(4) (2025) 197-212

Implementation and Comparison of Multi-motor Synchronization Control Strategies with a Distributed Topology

Nilay Şavklıyıldız [*], Övünç Polat

Department of Electrical-Electronic Engineering, Faculty of Engineering, Akdeniz University, Antalya, Türkiye

✉: *nilaytabanli@gmail.com**, *ovuncpolat@akdeniz.edu.tr* : *0009-0007-6533-8538 [*], 0000-0002-9581-2591 [b]*

Received: 30.08.2025 Revised: 04.10.2025, Accepted: 13.10.2025

Abstract

Multi-motor drive systems are widely used in modern applications that require precise synchronization of speed or torque, particularly when motors are mechanically coupled to a common load. A lack of proper coordination leads to unbalanced torques, mechanical stress, and vibrations, which ultimately reduce system efficiency. Maintaining reliable synchronization remains challenging due to system asymmetries and the limitations of conventional centralized or master–follower approaches. This study introduces a control strategy for three Permanent Magnet Synchronous Motors (PMSMs) rigidly coupled to a single shaft. In the experimental setup, three synchronization methods were implemented: Parallel, Torque-Follower, and the proposed Multilateral control. Each motor is driven by an independent controller and driver unit. Depending on the selected topology; these units perform either torque control or integrated velocity and torque control. Comparative results show that the proposed Multilateral control improves torque and velocity synchronization. It reduces mean squared errors compared to Torque-Follower method and provides more balanced torque distribution than Parallel under both no-load and loaded conditions. These findings show its potential as a scalable solution for advanced multi-motor applications.

Keywords: Permanent Magnet Synchronous Motor, Multi-Motor Synchronization, Multilateral Control, Torque-Follower Control, Parallel control.

1. Introduction

Multi-motor synchronization has become increasingly essential in applications such as robotics, electric vehicles, textile machines, and multi-axis machining. In these systems, coordinated motion among motors is more critical than the tracking accuracy of individual units. Synchronization ensures stable torque distribution and precise motion, especially in systems where multiple motors are mechanically coupled to a shared load [1,2]. Although rigid mechanical coupling is often used in multi-motor systems, physical linkage alone is insufficient to maintain synchronization [3]. In this context, a notable implementation of multi-motor synchronous control (MMSC) is in rigidly coupled electro-motor systems. These systems are widely used in industrial settings that demand high torque, reliability, and position or velocity accuracy, such as tunnel boring machines, antenna positioning mechanisms, and multi-source yaw control in wind turbines. [4–6]. In these systems, multiple motors transmit torque to a common gear structure. Although the speed and torque control of each motor can be effectively achieved with vector control techniques, coordinated operation among multiple mechanically coupled motors remains challenging. In demanding operating environments, often characterized by harsh working conditions, mechanical mismatches may cause a torque imbalance that can lead to motor overload and ultimately system-wide instability. Hence, ensuring effective coordination among rigidly coupled motors is fundamental for maintaining system stability, safety, and efficiency under practical operating conditions [4,6].

Digital MMSC strategies have been developed to overcome the inherent limitations of purely mechanical coupling. These approaches achieve synchronization through real-time information

exchange among controllers, enabling more reliable coordination and balanced load sharing in multi-motor systems, particularly within distributed control architectures [7]. Real-time communication in multi-motor systems is often realized through bus-based architectures. For instance, one study employed an MCU with CAN bus communication to the host and combined it with an FPGA for parallel processing, in order to accelerate multi-axis control and enhance real-time performance [8].

A variety of synchronization strategies, such as centralized, leader–follower, and distributed control architectures, have been developed to address the challenges of coordination and robustness in multi-motor systems [1]. In industrial applications such as packaging lines, conveyors, and flying shears, specific methods like Master–Slave, Cross Coupling, and Relative Coupling have been implemented, each offering distinct advantages depending on the system configuration and load conditions [9].

Recent studies have also emphasized coupling control strategies. For example, an enhanced deviation coupling control method for multi-motor rigid connection systems was proposed, where both speed and torque synchronization were compensated simultaneously, showing improved anti-disturbance performance and reduced synchronization errors [10]. In another approach, a fuzzy inference-based adjacent deviation coupling strategy was introduced, which strengthened robustness and improved cooperative synchronization accuracy [11].

Beyond rigid connection systems, recent years have seen growing interest in distributed permanent magnet direct-drive belt conveyor systems, employing a common synchronous speed reference together with a multi-motor ring coupling control strategy. This method demonstrated reduced tension increments, shorter start-up time, and improved robustness under local load disturbances compared with conventional single-motor conveyor systems [12].

Although synchronization is challenging, multi-motor systems offer practical advantages that a single large motor cannot provide. By distributing the mechanical load across multiple smaller motors, systems can achieve higher torque density, improve thermal performance, and reduce mechanical stress per motor [13]. This modularity also provides redundancy; if one motor fails, the others can compensate to maintain system functionality, which is particularly important in safety-critical applications. In addition to these advantages, the distributed nature of multi-motor systems enhances dynamic response and vibration suppression. It enables applying force at multiple locations and allows for flexible motor placement in spatially constrained environments such as humanoid robots or aerospace platforms [14].

Various synchronization strategies have been explored in the literature [1,9,15] , achieving precise alignment in position and velocity across motors remains a significant challenge, particularly when motors operate under different load conditions or exhibit structural asymmetries. As emphasized in [15], high-quality synchronous control cannot be achieved merely by minimizing the tracking error of each individual motor; instead, it requires an explicit coordination mechanism that actively reduces the relative errors between motors. In addition to traditional parallel or master–slave configurations, more recent strategies have introduced feedback-based and distributed coordination mechanisms to enhance inter-motor synchronization [16].

While existing MMSC approaches improve performance, further progress is required to meet modern demands. To address this, this study proposes a distributed control method designed to enhance coordination and load sharing. Three control strategies are implemented and compared: Parallel control, Torque-Follower control, and the proposed Multilateral control. Their respective advantages and limitations are analysed to provide a comprehensive understanding of multi-motor synchronization methods under varying operating conditions. Tests were

performed on a three-motor hardware testbed to evaluate performance across six distinct operating regions. These regions include acceleration, no-load constant speed, load application, constant speed with load, speed change, and constant low-speed with load A comparison with Parallel control showed that Multilateral control is more efficient, indicating that fully independent (Parallel) control of the motors is not a practical solution. Compared with Torque-Follower control, Multilateral improved speed synchronization notably in the steady-speed and load-application regions; however, current and torque errors were region-dependent, with Multilateral performing better in some regions and Torque-Follower in others. In addition, the proposed architecture is modular and supports real-time communication, allowing practical scalability to larger multi-motor systems.

2. Permanent Magnet Synchronous Motor Modelling

Understanding and comparing multi-motor strategies starts with single-motor modelling, which is the building block for multi-motor approaches. The Permanent Magnet Synchronous Motor (PMSM), widely used in high-performance drives, is modelled here as a single motor. A PMSM is commonly controlled with Field-Oriented Control (FOC) [17], which transforms measured three-phase currents into the rotating d–q frame, as illustrated in Fig. 1 [18]. The stator voltage equations in (1) and (2) describe resistance drops, flux dynamics, and speed-dependent terms.

$$u_q = R_s i_q + \frac{d\lambda_q}{dt} + n_p \omega_r \lambda_d \tag{1}$$

$$u_d = R_s i_d + \frac{d\lambda_d}{dt} - n_p \omega_r \lambda_q \tag{2}$$

In these equations, u_d and u_q denote the stator voltages in the d and q axes, similarly, each i represents the corresponding stator current components, and each λ represents the flux linkage components. Rs is the stator resistance, n_p is the number of pole pairs, and ω_r is the electrical rotor speed.

Equations (3) and (4) express the flux linkages in terms of stator currents, where the permanent magnet flux is ϕ_e. L_q and L_d represent the d and q-axis inductances. These equations allow torque and flux to be controlled separately.

$$\lambda_q = L_q i_q \tag{3}$$

$$\lambda_d = L_d i_d + \phi_e \tag{4}$$

The transformation from three-phase quantities to the α–β and subsequently to the d–q reference frame is performed using Clarke-Park transforms, as given in Eq. (5), (6), and (7).

$$\begin{bmatrix} i_\alpha \\ i_\beta \\ i_0 \end{bmatrix} = \begin{bmatrix} 2/3 & -1/3 & -1/3 \\ 0 & 1/\sqrt{3} & -1/\sqrt{3} \\ 1/3 & 1/3 & 1/3 \end{bmatrix} \begin{bmatrix} i_a \\ i_b \\ i_c \end{bmatrix} \tag{5}$$

$$\begin{bmatrix} i_d \\ i_q \\ i_0 \end{bmatrix} = \begin{bmatrix} \cos\theta & \sin\theta & 0 \\ -\sin\theta & \cos\theta & 0 \\ 0 & 0 & 1 \end{bmatrix} \begin{bmatrix} i_\alpha \\ i_\beta \\ i_0 \end{bmatrix} \tag{6}$$

$$\begin{bmatrix} i_\alpha \\ i_\beta \\ i_0 \end{bmatrix} = \begin{bmatrix} \cos\theta & -\sin\theta & 0 \\ \sin\theta & \cos\theta & 0 \\ 0 & 0 & 1 \end{bmatrix} \begin{bmatrix} i_d \\ i_q \\ i_0 \end{bmatrix} \tag{7}$$

The electromagnetic torque of a PMSM can be expressed by Eq. (8), where k_t is the torque constant and i_q is the q-axis current. This relationship enables torque control in the FOC framework by regulating i_q, under the assumption that $i_d \approx 0$. Conventionally, experimental torque-related interpretations are based on the measured i_q values. Accordingly, the torque behaviour observed in experimental results is interpreted through the measured i_q values.

$$T = \frac{3}{2} k_t i_q = \frac{3}{2} k_t I_{pk} \tag{8}$$

$$k_t = n_p \phi_e \tag{9}$$

The torque constant k_t represents the peak torque produced per phase current and is numerically identical to the back-EMF constant k_e when both are expressed in SI units ($k_t = n_p \phi_e = k_e$).

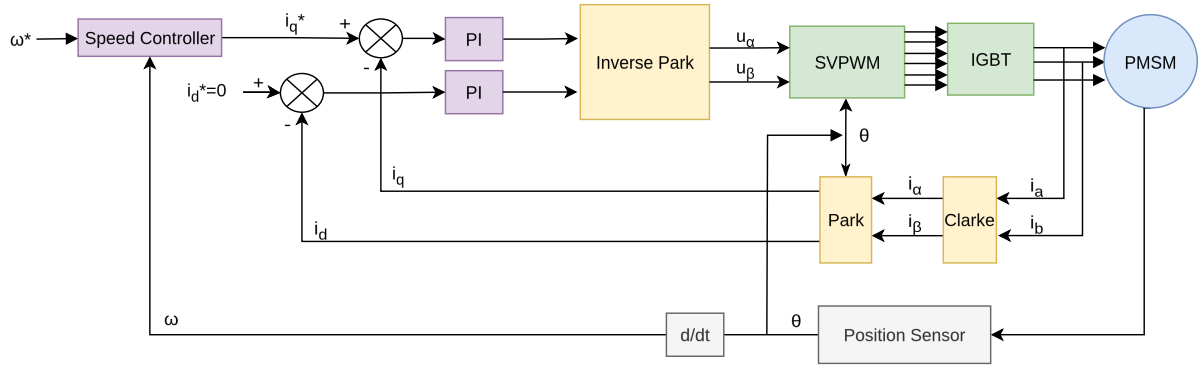

Fig. 1. Overall control structure of PMSM drive system based on Field-Oriented Control

3. Multi-Motor Control Strategies

Multi-motor systems require synchronization when several motors drive a shared mechanical load. Control strategies differ in reference generation, feedback utilization, and coordination among motors. Parallel and Torque-Follower control strategies are fundamental examples of these approaches, while the proposed Multilateral control in this study provides a distributed alternative [1]. These strategies are illustrated in Fig. 2.

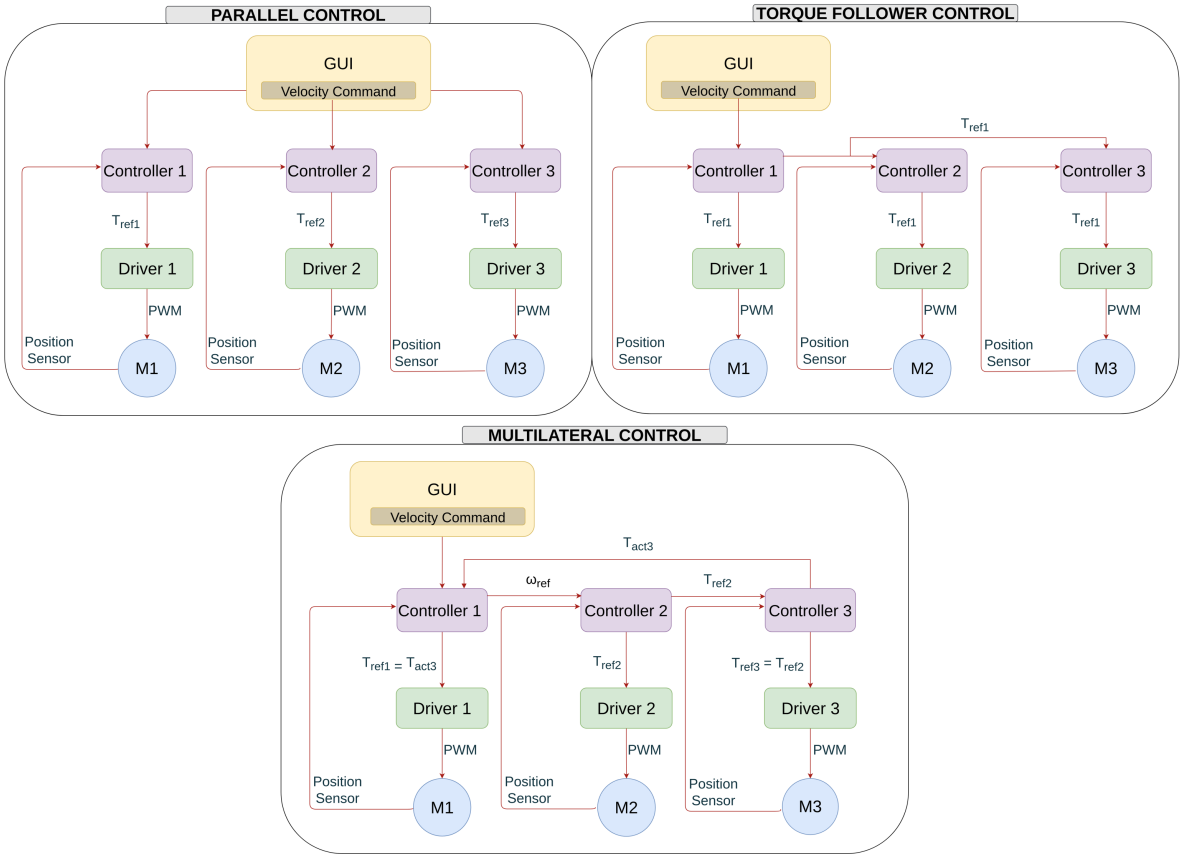

Fig. 2. Parallel, Torque-Follower, and Multilateral control strategies

3.1. Parallel Control

In the Parallel control strategy, each motor operates completely independently based on its own velocity reference signals. All motors execute cascaded control loops, typically consisting of velocity and FOC (torque and flux control), without any exchange of information between them. In the considered system, each of the three Permanent Magnet Synchronous Motors (PMSMs) is paired with a dedicated controller–driver unit and performs full local control using only its own feedback. While this structure provides modularity, ease of implementation, and hardware flexibility, it does not account for the dynamic interactions among motors mechanically coupled to the same load [10,15].

3.2. Torque-Follower Control

In the Torque-Follower control approach, a hierarchical architecture is established where one motor is assigned as the master and the others act as slaves or followers [19]. The master motor executes the complete cascaded control loop, including velocity, and torque control and generates a single torque reference. This reference is broadcast to the follower motors, which perform only torque control using their own Field-Oriented Control (FOC) loops. As a result, all motors apply the same torque command, allowing them to operate in synchronously without executing local velocity control.

This strategy is relatively simple to implement and achieve basic coordination under balanced and steady operating conditions. However, follower motors do not consider their own dynamic state, such as speed or load interaction [20].

3.3. Multilateral Control

The term “Multilateral” in this study refers to a control structure where each motor not only receives local feedback but also dynamically adjusts its control action based on the real-time motion reference and torque output of the other motors. Unlike centralized or master–follower approaches where coordination is imposed in a unidirectional or hierarchical structure, the proposed method establishes a mutually interactive, fully distributed feedback loop among all motor controllers. This enables synchronized operation through shared load awareness and coordination [21,22]. The Multilateral Control strategy introduces a distributed and cooperative architecture for multi-motor synchronization. In this method, coordination is achieved through mutual exchange of motion references and torque feedback between controllers, enabling all motors to operate with real-time awareness of the common load. In the present system, the motion reference is defined as the velocity command; however, position reference could also be employed depending on the application requirements.

In the proposed Multilateral control strategy, the three controllers are interconnected in a ring topology, enabling real-time torque feedback between units. Controller 1 receives the velocity commands from the PC and computes the corresponding velocity references based on a third-order trajectory generation scheme. It also performs torque control by taking the actual torque value from Controller 3 as its reference. Controller 2 performs full cascaded control (velocity and torque) using the references from Controller 1. Controller 3 performs only torque control, with its torque reference taken directly from the torque reference generated by Controller 2. This closed-loop ring topology aims for mutual torque influence among all controllers, adaptive load sharing, and improved synchronization performance under varying load conditions.

4. Experimental Setup and Methodology

The experimental test platform consists of three 24 V, 5 Nm Permanent Magnet Synchronous Motors (PMSM), each driven by an independent controller-driver board. Each controller–driver board consists of a microcontroller unit (MCU) responsible for control and communication tasks. Every motor is equipped with its own high-resolution rotary encoder for precise position and velocity feedback. Phase currents are measured using low-resistance shunt resistors and digitized by a 12-bit ADC at a fixed sampling rate. The system also incorporates a centrally located torque sensor, which is mounted on the common shaft connecting the motors. An electromagnetic brake is also integrated into the setup to apply controllable load conditions during testing. Table 1 summarizes the technical specifications of the test hardware, including PMSM, position sensor, torque sensor, and electromagnetic brake. The controller and driver boards communicate via a 1 Mbit/s CAN Bus network to establish a modular and distributed control architecture. This communication supports real-time data exchange among the controllers. A Graphical User Interface (GUI) on a host PC communicates with the controllers via Ethernet (100 Mbit/s), allowing start/stop actions, sending trajectory parameters (velocity, angular acceleration command), and data logging. The overall architecture of the distributed control platform is shown in Fig. 3**.**

Table 1. Technical specifications of the PMSM, torque sensor, and electromagnetic brake used in the experimental setup

Devices	Specifications	Description
Motor	Model	140TAST-01T4M44K
	Rated Voltage	24 V
	Rated Power	157 W
	Rated Torque	5.0 Nm
	Rated Speed	300 rpm
	Rated Current	8.0 A
	Moment of Inertia	28.7 x10^{-4} kg.m^2
	Pole Number	20
Position Sensor	Type	14-bit magnetic rotary encoder
	Interface	ABI incremental output
	Resolution	4096 steps per revolution
	Max. Rotary Speed	Up to 28 krpm
Torque Sensor	Model	8661-5050-V0200
	Name	High-Precision Rotating-Contactless Torque Sensor
	Measuring Range	±50 Nm
	Refresh Rate	2000 measurements/s
	Linearity Deviation	≤ ±0.05 % F.S.
Brake	Model	ABTF-03
	Max. Current/Voltage	1 A, 24 V
	Max. Brake Torque	35 Nm Electromagnetic Powder Brake

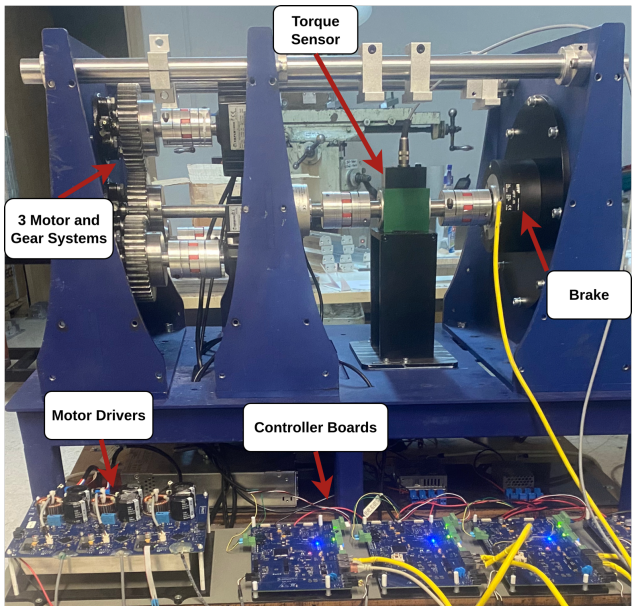

a) Front view of motors, drivers, controllers, torque sensor, and brake

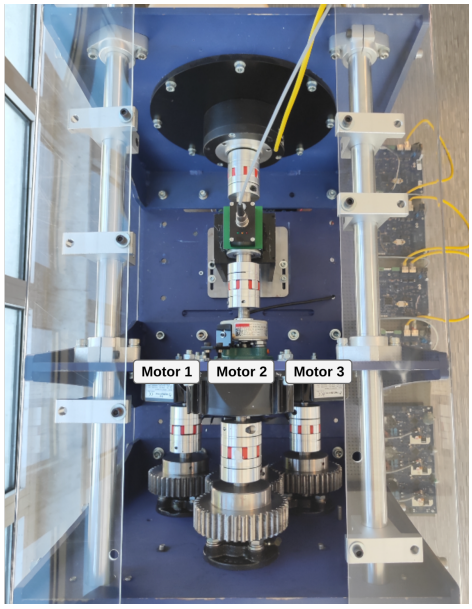

b) Top view of the three-motor gear coupling

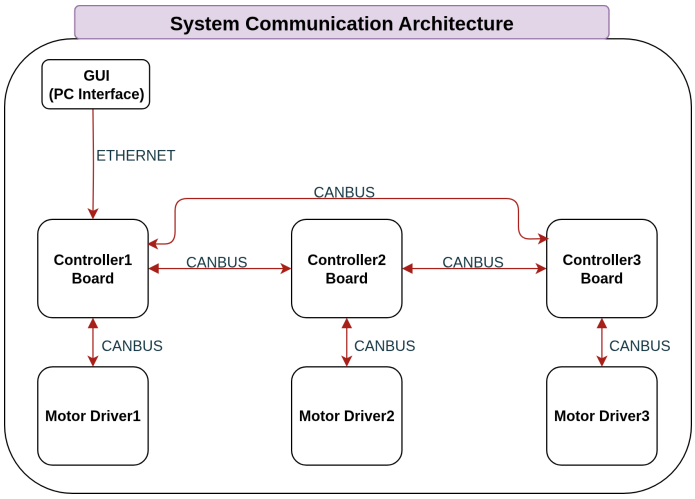

c) System communication architecture

Fig. 3. Experimental multi-motor test bench

5. Experimental Results

Characterizing the PMSM drive system requires an initial validation of the linear relationship between current and torque. To validate the linear relationship between the q-axis current (I_q) and the generated torque, a static test was implemented with the torque sensor. The expected torque for each test case was calculated from the measured I_q values, based on the torque equation given in Eq. (8) and the known torque constant of the PMSM. Tests were performed sequentially with one, two, and three motors connected to the common shaft. To ensure maintain static conditions, the electromagnetic brake was set to a torque level higher than the combined capability of the motors. This configuration effectively prevented any shaft rotation. This setup allows simultaneous verification of both hardware and control software functionality, and the test was implemented using the Parallel control strategy to prove the integrity of the overall system architecture.

Two complementary static bench tests were then performed to further confirm torque estimation accuracy and evaluate torque sharing. In the Constant-Current Test, a fixed I_q command was set as the reference. During this test the number of active motors was changed, and the measured torque values were compared with the theoretical ones (see Table 2). In the Constant-Torque, the total torque was intended to be maintained constant by adjusting the I_q according to the number of motors. Both tests confirmed that the control system distributes torque evenly across motors and the torque–I_q relationship remains consistent under different test conditions.

Table 2. Static torque verification tests: Constant-Current and Constant-Torque

Test	*Number of Motors*	*Motor I_q Current (A)*	*Estimated Torque (Nm)*	*Measured Torque (Nm)*
Constant-Current (5A)	1	5.00	2.15	2.15
	2	5.00	4.30	4.30
	3	5.00	6.45	6.50
Constant-Torque (5A)	1	5.00	2.15	2.15
	2	2.50	2.15	2.10
	3	1.67	2.15	1.90
Constant-Torque (7A)	1	7.00	3.01	3.00
	2	3.5	3.01	2.80
	3	2.33	3.01	2.90

Brake Current: 0.5 (A); Brake Torque: 17.50 (Nm)

5.1. Parallel Control Performance

The Parallel control method was initially examined to verify its reliability and performance in achieving stable current or torque distribution and synchronized operation over extended steady-state conditions. A constant speed reference of 21 rad/s was applied without external braking load, with the expectation that phase currents would remain constant under steady-state operation.

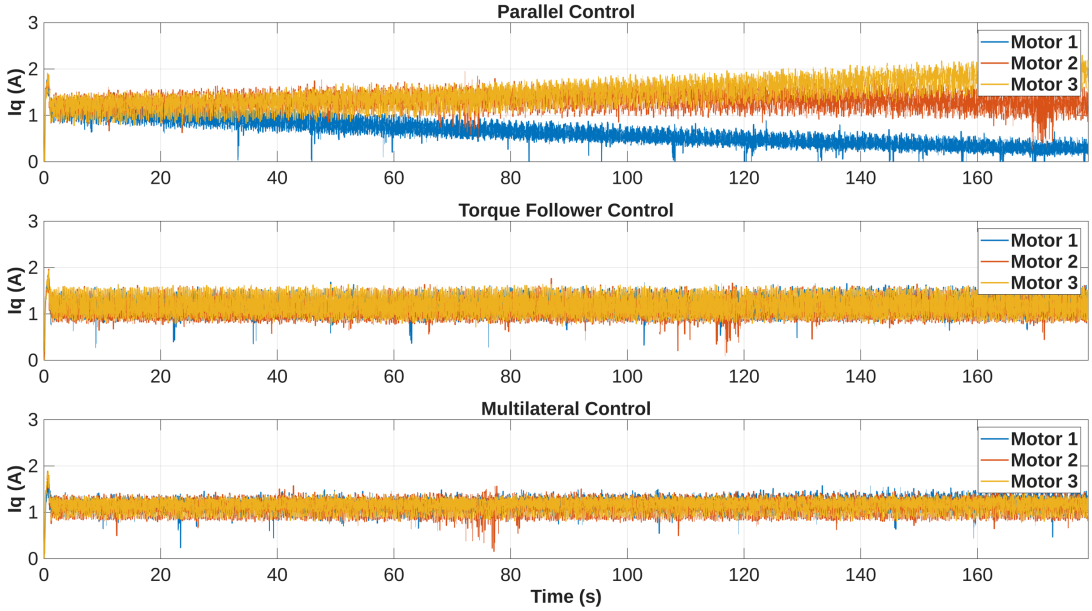

Fig. 4. Current tracking performance of the Parallel, Torque-Follower, and Multilateral control at 21 rad/s with no load

As shown in Fig. 4, under the Parallel control strategy, the current responses showed a progressive imbalance in current distribution: the current in Motor 1 gradually decreased over time, the current in Motor 3 increased over time, while Motor 2 remained relatively stable. In contrast, both the Multilateral and Torque-Follower strategies maintained stable phase currents across all motors under identical test conditions. This imbalance in the Parallel configuration shows unequal torque production among the motors and the limitation of this approach in continuous operation. The observations were consistently reproduced across multiple experimental repetitions, confirming the consistency of the results. Additional tests with two-motor configurations (e.g., M1–M3 and M2–M3 pairs) further demonstrated similar unbalanced load distributions under Parallel control. As a result, while Parallel control can serve as a baseline, it is unsuitable for real-world implementation in rigidly coupled multi-motor systems due to current deviation and unstable torque sharing.

5.2. Region-based Analysis of Multilateral and Torque-Follower Control

For the comparative evaluation of the Multilateral and Torque-Follower strategies, the experimental setup was driven according to a predefined test profile, shown in Fig. 5. The trajectory is divided into predefined regions to evaluate system performance under different operating conditions: acceleration, no-load constant speed, load applied, constant speed with load, speed change, and constant low-speed with load.

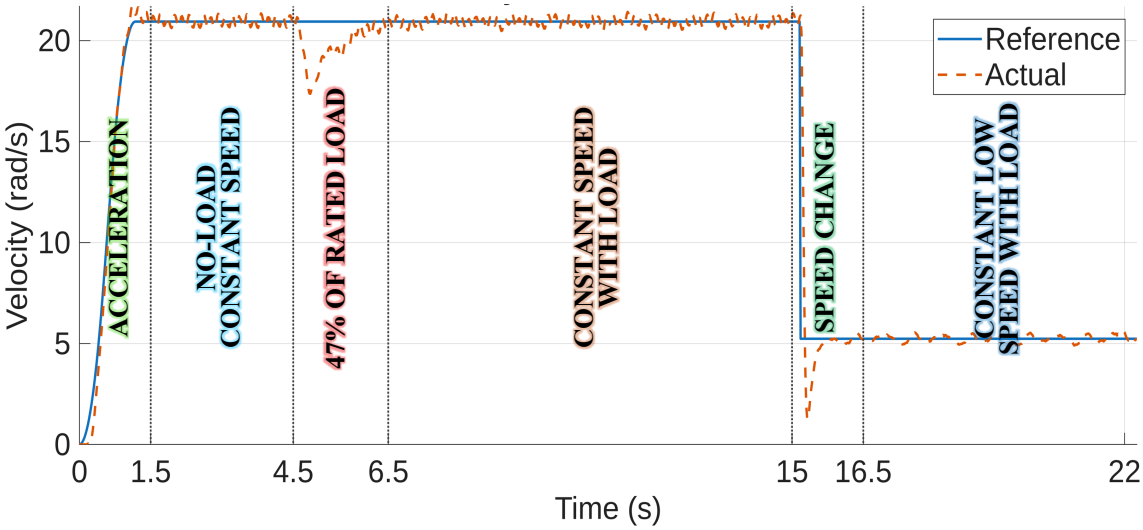

Fig. 5. Driving regions in velocity reference and velocity actual parameters

The motors were first accelerated to a no-load constant speed of 21 rad/s. At t = 5 s, a 7.0 Nm brake load was applied and maintained until the end of the test. At t = 15 s, the reference speed was reduced from 21 rad/s to 6 rad/s, and the system response was observed. The total applied load of 7.0 Nm was distributed equally among the three motors, resulting in approximately 2.33 Nm per motor (≈47% of the motor rated torque, 5.0 Nm).

Fig. 6 compares the velocity and current responses of the three motors under Multilateral and Torque-Follower control. In both strategies, it is difficult to evaluate synchronization performance directly from these plots; the graphs only can show velocity and current profiles of the drive system. Therefore, the comparisons are based on error signals and mean squared error (MSE) values, which provide a clearer measure of synchronization and load-sharing performance.

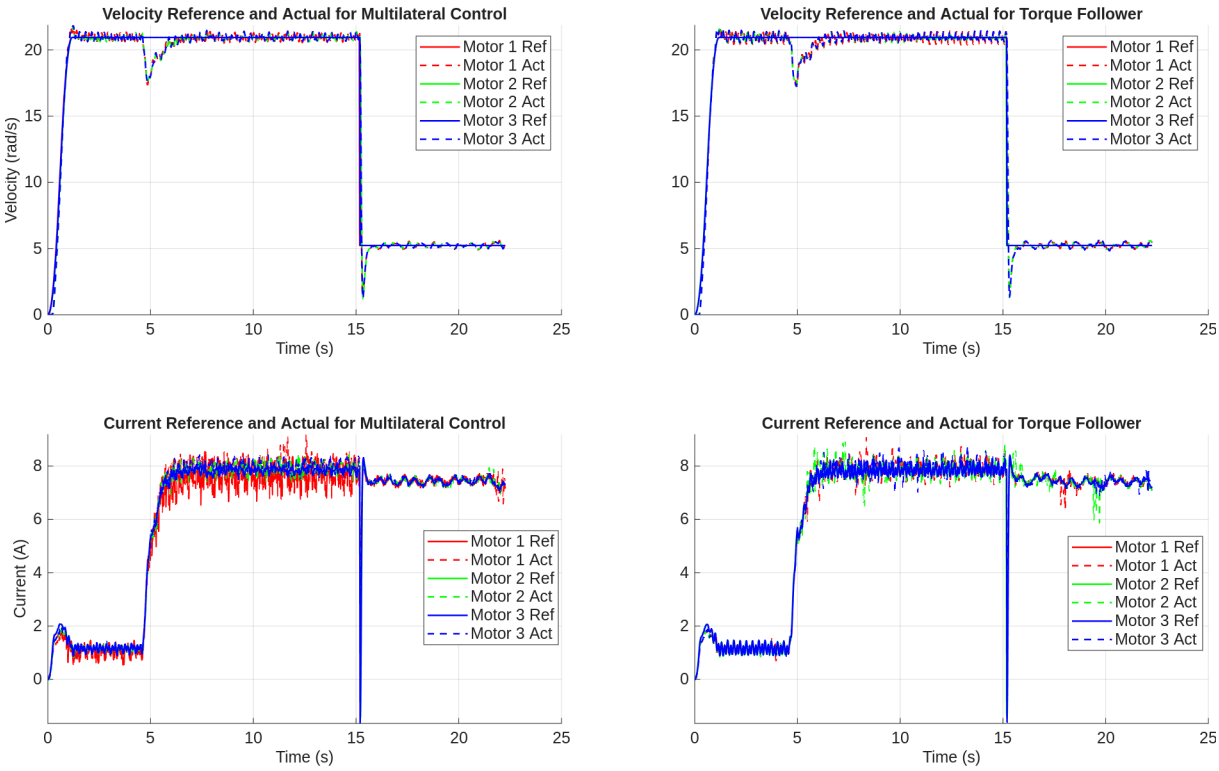

a) Multilateral Control b) Torque-Follower Control

Fig. 6. Current and velocity reference and actual responses of three motors

Tracking errors for velocity and current are examined both as instantaneous error signals (see Fig. 7–8) and mean square error (MSE) values (see Eq. 9). The velocity error is defined as $\omega_{ref} - \omega_{actual}$, where ω_{ref} is generated by the trajectory generator andω_{actual} is obtained from encoder measurements. The current error is defined as $i_{q_{ref}} - i_{q_{actual}}$, with $i_{q_{actual}}$measured from the motor phase currents. Within the Field-Oriented Control (FOC) framework, the electromagnetic torque is expressed by Eq. (8), which indicates that the current error is directly proportional to the torque error through the torque constant Kt. The torque reference used in the block diagrams also corresponds to $i_{q_{ref}}$ scaled by the torque constant Kt.

$$MSE = \frac{1}{N}\sum_{i=1}^{N}(x_i - \hat{x}_i)^2 \tag{9}$$

Three consecutive experimental tests were performed, and the mean squared error (MSE) values in Table 3 were calculated as the average across these tests to provide a basis for quantitative comparison of the control strategies.

In the region-based comparison, the Multilateral control shows better performance across all motors in the no-load constant speed, constant low-speed with load, and load-applied regions, giving lower velocity errors than Torque-Follower. In the speed change regions, Motor 2 achieves better results with Multilateral, whereas Torque-Follower provides lower velocity errors in Motor 1 and Motor 3.

When current/torque errors are considered, Motor 2 and Motor 3 perform better with the Multilateral control in most regions, showing lower error values. On the other hand, Torque-

Follower shows lower current errors for Motor 1, but this outcome is mainly related to the fact that its torque reference was derived from the actual torque of Motor 3, introducing a measurement-dependent bias in the results.

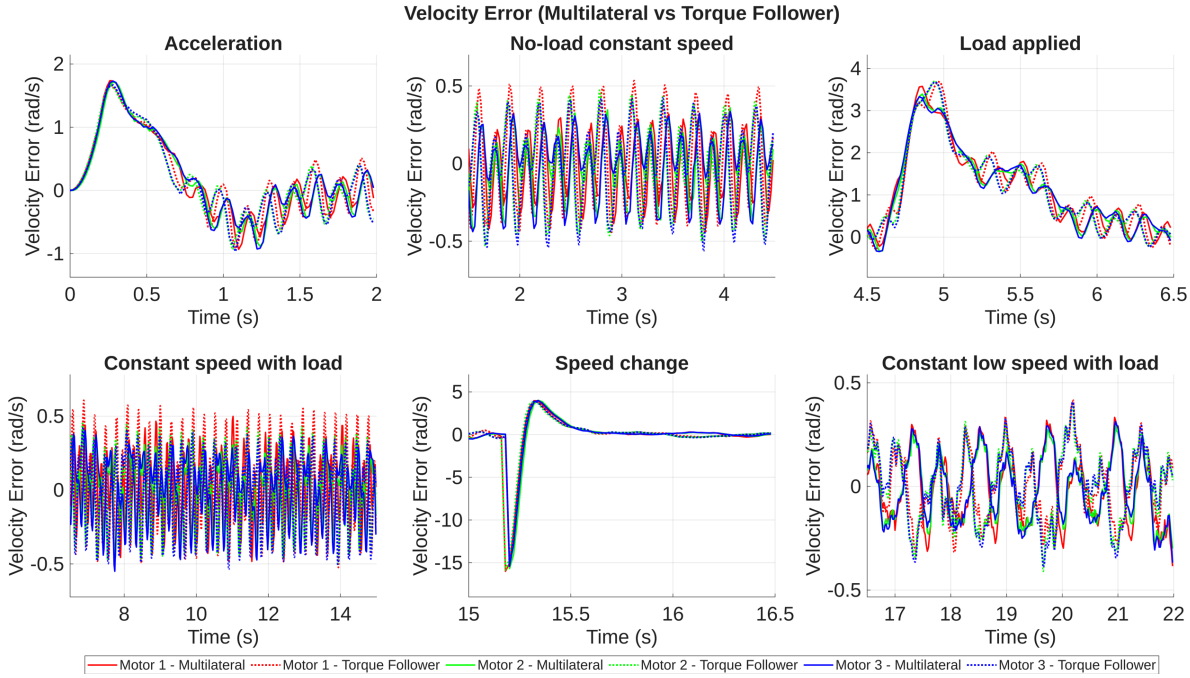

Fig. 7. Velocity error responses of motors under Multilateral and Torque-Follower strategies

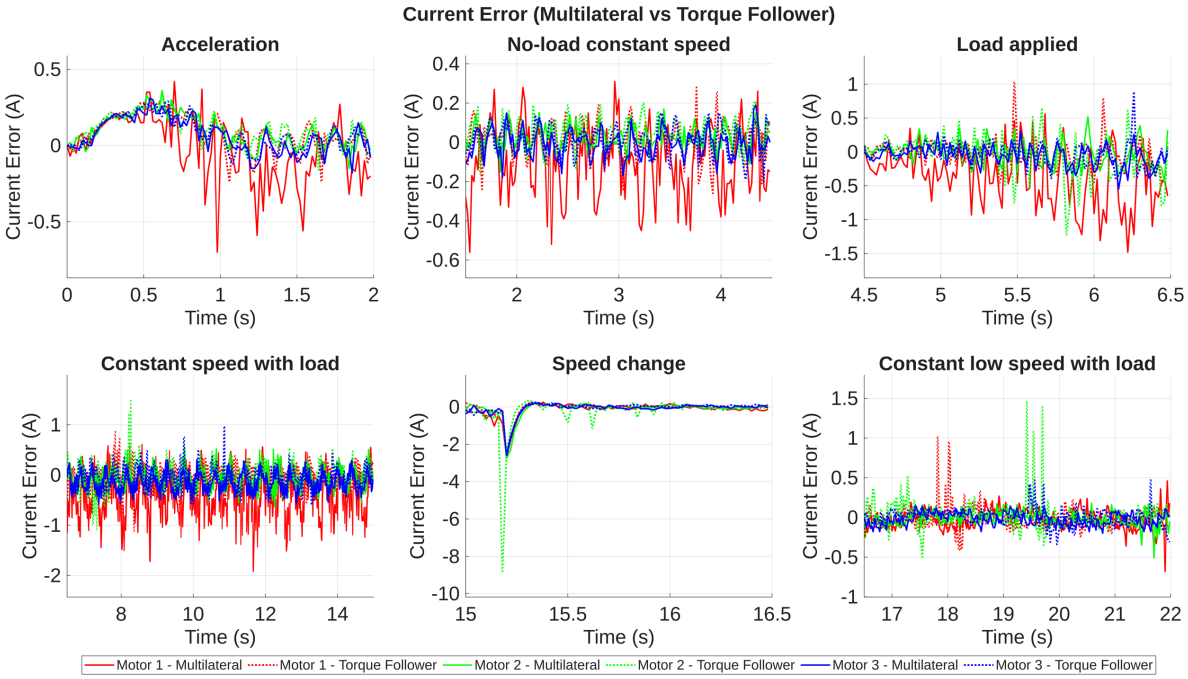

Fig. 8. Current error responses of motors under Multilateral and Torque-Follower strategies

Table 3. Average velocity and current MSE values for Multilateral and Torque-Follower control across driving regions, where the lowest values are highlighted

	Region	Velocity Error		Current Error	
		Multilateral	**Torque Follower**	**Multilateral**	**Torque Follower**
Motor #1	Acceleration	0.652027	0.576514	0.036196	0.025921
	No-load constant speed	0.043920	0.083313	0.019601	0.008000
	Load applied	2.296792	2.356323	0.162499	0.036732
	Constant speed with load	0.046555	0.082676	0.177080	0.071448
	Speed Change	9.454445	7.017653	0.230518	0.168186
	Constant low-speedwith load	0.024967	0.026824	0.017138	0.014052
Motor #2	Acceleration	0.621854	0.582056	0.028680	0.025555
	No-load constant speed	0.037769	0.067928	0.009451	0.006729
	Load applied	2.288399	2.340192	0.063717	0.056130
	Constant speed with load	0.030104	0.059416	0.053166	0.057045
	Speed Change	8.393957	8.750877	0.536160	1.243575
	Constant low-speedwith load	0.021975	0.029859	0.010183	0.015714
Motor #3	Acceleration	0.645571	0.585451	0.022371	0.021312
	No-load constant speed	0.044890	0.075691	0.004100	0.006452
	Load applied	2.292786	2.349705	0.024444	0.027163
	Constant speed with load	0.038831	0.069290	0.046747	0.047182
	Speed Change	8.569537	6.129741	0.345427	0.152790
	Constant low-speedwith load	0.023228	0.032768	0.005767	0.007265

The comparison indicates that Torque-Follower can achieve lower errors in specific speed change conditions and in Motor 1's current response. Nevertheless, Multilateral control performs better in the majority of operating regions, particularly under steady-state and load conditions, it achieves lower velocity and current errors and provides a more balanced torque distribution among the motors.

Beyond the comparative performance results, it is also important to highlight the structural advantages of the proposed architecture. The proposed architecture does not require motors to be placed adjacent, despite operating on a common mechanical load. For example, in a long conveyor system, motors can be distributed along different segments of the line [23]. Through communication between controllers, synchronization and torque sharing can still be achieved across the system. This results in a physically distributed yet dynamically integrated control structure, offering high adaptability in applications such as modular production lines, long-range transport systems, or coordinated lifting platforms. This modular and distributed architecture provides a flexible platform for evaluating and deploying multi-motor coordination strategies in high-performance applications [24].

To support modular, scalable, and high-precision control, the system architecture adopts a fully distributed hardware design, where each motor is driven by its own dedicated controller and driver units. This configuration provides several system-level advantages [25] First, it enables full modularity; each motor unit can be independently developed, tested, updated, or replaced without affecting the rest of the system. Second, the architecture supports local control capability, where each controller acquires its own sensor data, executes position, velocity, and torque control algorithms in real time, and communicates with other controllers when coordination is required. This allows the implementation of feedback-based synchronization schemes without relying on a centralized processing unit. In addition, the use of high-resolution sensing and per-motor cascaded control loops enables precise regulation of motion and torque. Finally, the system is easily extensible: new motors can be added by integrating additional controller driver pairs, without altering the existing control infrastructure.

6. Conclusions

This study experimentally compared three control strategies for rigidly coupled PMSMs: Parallel, Torque-Follower, and the proposed Multilateral control. The comparison showed that; while the Parallel control method is a common baseline, it exhibited current deviation and unbalanced torque sharing thus limiting its practical applicability. Torque-Follower achieved lower errors specifically during acceleration and speed change phases, and for one motor's current response. However, its effectiveness was limited to specific operating conditions. In contrast, the Multilateral control provided lower velocity and current errors across most regions, particularly under steady-state conditions and when a load was applied. Its improved synchronization performance is especially important for multi-motor driven industrial applications.

Through this comparative evaluation, the Multilateral control proved to be a scalable and reliable strategy for multi-motor synchronization, addressing the shortcomings of conventional parallel and master–follower approaches. Future research could expand this framework to a larger number of motors, include different motor types, and under failure conditions to further assess robustness.

Author Contribution

Nilay Şavklıyıldız: Conceptualization; Data curation; Investigation; Methodology; Software; Visualization; Writing—original draft; Writing—review & editing.

Övünç Polat: Conceptualization; Investigation; Methodology; Resources; Supervision; Validation; Writing—original draft; Writing—review & editing.

Acknowledgement

The authors would like to express gratitude to Desird Design R&D for providing access to the experimental platform used in this study.

References

[1] Niu, F., Sun, K., Huang, S., Hu, Y., Liang, D., Fang, Y., A Review on Multimotor Synchronous Control Methods. *IEEE Transactions on Transportation Electrification*, 9, 22–33, 2023.

[2] Sun, D., Mills, J.K., Adaptive synchronized control for coordination of multirobot assembly tasks. *IEEE Transactions on Robotics and Automation*, 18, 498–510, 2002.

[3] Kong, X., Chen, X., Dou, J., Zhang, X., Wen, B., Controlled Synchronization of Two Nonidentical Homodromy Coupling Exciters Driven by Inductor Motors in a Vibratory System. *Proceedings of the Institution of Mechanical Engineers Part C Journal of Mechanical Engineering Science*, 230, 3040–3054, 2016.

[4] Liu, T., Chen, C., Ye, B., Chen, Y., Comparative study of the synchronous control for rigidly coupled electro-motors. *Journal of Physics: Conference Series*, 1983, 012065, 2021.

[5] Wei, J., Sun, Q., Sun, W., Ding, X., Tu, W., Wang, Q., Load-sharing characteristic of multiple pinions driving in tunneling boring machine. *Chinese Journal of Mechanical Engineering*, 26, 532–540, 2013.

[6] Dai, J., He, T., Li, M., Long, X., Performance study of multi-source driving yaw system for aiding yaw control of wind turbines. *Renewable Energy*, 163, 154–171, 2021.

[7] Yu, G., Sun, J., Wu, Z., Liu, H., Ji, W., Research on a Multi-Motor Coordinated Control Strategy Based on Fuzzy Ring Coupling Control. 2020 Chinese Automation Congress (CAC), 2020.

[8] Gou, M., Wang, B., Zhang, X., Development of Multi-Motor Servo Control System Based on Heterogeneous Embedded Platforms. *Electronics*, 13, 2024.

[9] Perez-Pinal, C. Nunez, R. Alvarez, I. Cervantes, Comparison of multi-motor synchronization techniques. 30th Annual Conference of IEEE Industrial Electronics Society, 2004. IECON 2004, 2004.

[10] Jiang, C., Fan, B., Hong, Q., Dong, J., Sun, L., Synchronization and coordination control based on enhanced deviation coupling for multi-motor rigid connection systems. Engineering *Research Express*, 7, 015340, 2025.

[11] Hang, C., Tan, Y., Li, R., Research on Cooperative Control Strategy of Multi-Motor System Based on Fuzzy Inference. *Journal of Physics Conference Series*, 2187, 012002, 2022.

[12] Zhou, Q., Gong, H., Du, G., Zhang, Y., He, H., Distributed Permanent Magnet Direct-Drive Belt Conveyor System and Its Control Strategy. *Energies*, 15, 2022.

[13] Gong, C., Li, Y.R., Zargari, N.R., An Overview of Advancements in Multimotor Drives: Structural Diversity, Advanced Control, Specific Technical Challenges, and Solutions. *Proceedings of the IEEE*, 112, 184–209, 2024.

[14] Sakka, M.A., Geury, T., Dhaens, M., Sakka, M.A., Baghdadi, M.E., Hegazy, O., Reliability and Cost Assessment of Fault-Tolerant Inverter Topologies for Multi-Motor Drive Systems. 2021 23rd European Conference on Power Electronics and Applications (EPE'21 ECCE Europe), 2021.

[15] Zhang, X., Hu, H., Wang, H., Wang, Z., Overview of position synchronous control technology for multi-motor system. *Systems Science & Control Engineering*, 12, 2427074, 2024.

[16] Zhou, Q., Shi, K., Xu, K., Du, G., Gao, K., Optimized Multi-Motor Power Control Strategy for Distributed Permanent Magnet Direct Drive Belt Conveyors. *Applied Sciences*, 14, 2024.

[17] Cordeiro, A., Manuel, J.F.M., Pires, V.F., Performance of synchronized master-slave closed-loop control of AC electric drives using real time motion over ethernet (RTMoE). *Mechatronics*, 69, 102400, 2020.

[18] Vas, P., Sensorless vector and direct torque control., Sensorless vector and direct torque control. Oxford university press, 1998.

[19] Lee, H.-J., Oh, K.-K., Comparison study of parallel operation of motor drives. 2017 17th International Conference on Control, Automation and Systems (ICCAS), 2017.

[20] Gao, S., Wang, Q., Li, G., Li, Z., Qian, Z., Zhang, Q., Diao, K., A review of multi-motor coordinated control technologies: advanced strategies, intelligent algorithms, and future trends. *Renewable and Sustainable Energy Reviews*, 225, 116188, 2026.

[21] Kebude, D., Morimitsu, H., Katsura, S., Sabanovic, A., Multilateral control-based motion copying system for haptic training. 2014 IEEE 23rd International Symposium on Industrial Electronics (ISIE), 2014.

[22] Kitamura, K., Yashiro, D., Ohnishi, K., Estimation and share of environmental impedance using multiple robots for haptic broadcasting. 2009 IEEE International Conference on Industrial Technology, 2009.

[23] Kovalchuk, M.S., Baburin, S.V., Modelling and control system of multi motor conveyor. *IOP Conference Series: Materials Science and Engineering*, 327, 022065, 2018.

[24] Huang, Z., Qiu, S., Wang, B., Liu, Q., A real-time field bus architecture for multi-smart-motor servo system. *Scientific Reports*, 14, 3918, 2024.

[25] Mitrovic, N., Kostić, V., Petronijevic, M., Jeftenic, B., Multi-Motor Drives for Crane Application. *Advances in Electrical and Computer Engineering*, 9, 2009.